Impact of ambient humidity on surface acoustic wave attenuation and velocity in hematoporphyrin-on-$LiNbO_3$ structure

R. Rimeika[1], R. Rotomskis[2], V. Poderys[2], D. Čiplys[1,3], A. Sereika[1] and M. S. Shur[3]

[1]Department of Radiophysics, and [2]Biophotonics Group, Laser Research Centre, Physics Faculty, Vilnius University, Saulėtekio 9, LT-10222 Vilnius, Lithuania

[3]Center for Integrated Electronics and Department of Electrical, Computer, and Systems Engineering, Rensselaer Polytechnic Institute (RPI), 110 8th Str., Troy, NY 12180, USA

Abstract

The impact of ambient humidity on a surface acoustic wave (SAW) propagation in the structure consisting of hematoporphyrin (Hp) film deposited on a piezoelectric lithium niobate substrate has been studied. The SAW transmission dependencies on frequency were measured using an RF network analyzer, and the variation in the SAW velocity was measured using SAW delay-line oscillator technique. The increase in the SAW velocity and decrease in the SAW attenuation with increasing ambient humidity was observed. Both dependencies exhibited exponential dependence on a humidity, and the relative velocity change was proportional to the squared change in the attenuation. This observation is in agreement with the conductivity related mechanism of the humidity impact on the SAW propagation parameters in a hematoporphyrin-lithium niobate structure. The results show that Hp - $LiNbO_3$ structure can be used as a SAW humidity sensor.

Keywords: surface acoustic wave, hematoporphyrin, humidity sensor.

Air humidity is a very important parameter for many application areas, such as automotive industry, food processing, meteorology, semiconductor technology, civil engineering and construction, medicine and health care. Conventional techniques of humidity measurements comprise mechanical and chilled mirror hygrometers, wet and dry bulb psychrometers, and infrared (IR) optical absorption hygrometers. With the advent of fiber optics (FO) technology, various FO-based techniques, including direct spectroscopic, evanescent wave, in-fiber grating and interferometric methods, have been applied for a humidity sensing [1]. The dominating role in development of humidity sensors belongs to electronic technologies, which allow implementation of low cost, reliable and compact devices based on capacitive, resistive and gravimetric methods [2]. Surface acoustic wave (SAW) humidity sensors use variations in SAW velocity or attenuation caused by the humidity-induced changes in mass density, viscoelastic properties, electric conductivity or dielectric properties of propagation medium [3]. The SAW sensors have a higher sensitivity than resistive and capacitive sensors [4]. Typical SAW humidity sensors use various polymer films as humidity-sensitive materials [5]. Recently, we have demonstrated the applicability of porphyrin family materials for implementation of SAW humidity sensors [6]. The important advantage of such a sensor was its high response and recovery speed in the sub-second range [7]. This was a motivation to investigate the suitability of another family material, hematoporphyrin (Hp), for use in SAW humidity sensors. In the present paper, we report on the impact of ambient humidity on the SAW attenuation and velocity in a hematoporphyrin-on-$LiNbO_3$ structure.

Hematoporphyrin (see Fig. 1) was first isolated from blood in 1867. It is a tetrapyrrole aromatic macrocycle, derivatives of which have been used for photodynamic treatment of cancerous tumors.

A sample under investigation consists of an *YZ* $LiNbO_3$ substrate with a deposited Hp film as shown in Fig. 2. A pair of Al-film interdigital transducers (IDTs) for SAW excitation and reception was deposited on the substrate by photolithography. The IDT period was 40 μm, the aperture was 2 mm, the number of electrode pairs $N = 20$, and center-to-center spacing of IDTs was 12 mm.

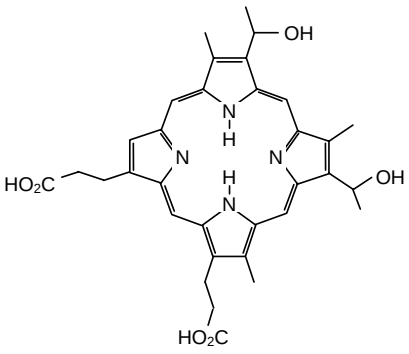

Fig. 1. **Hematoporphyrin molecule**

The hematoporphyrin powder (Sigma-Aldrich, USA) was dissolved in distilled water and further diluted until the concentration of $2 \cdot 10^{-4}$ mol/l was obtained. Optical spectroscopy measurements of this solution were performed using the Cary the 50 (Varian, Inc.) spectrophotometer. Fig. 3 shows the characteristic Soret band in the optical absorption spectrum of the solution. Its peak at 375 nm is blue-shifted with respect to that of a

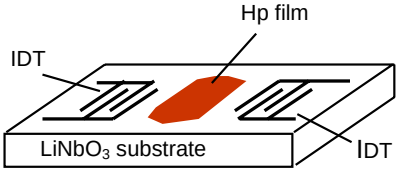

Fig. 2. **Hematoporphyrin-on-$LiNbO_3$ structure**

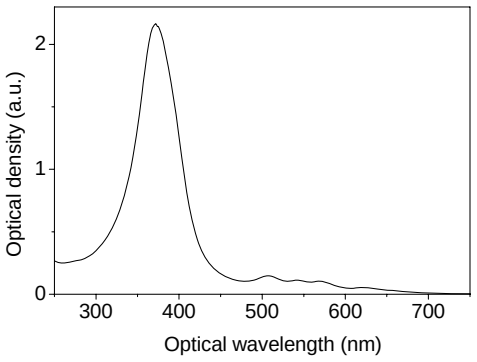

Fig. 3. **Soret band in the optical absorption spectrum of Hp solution with concentration $2 \cdot 10^{-4}$ mol/l**

monomeric Hp solution. It is known that the blue shift of the Soret band is related with arrangement of hematoporphyrin monomers into face-to-face aggregates (H-aggregates) [8]. The Hp film was deposited on the SAW propagation path between the IDTs as follows: an amount of 10 – 20 μl of the prepared solution was dropped on the substrate surface and dried at a room temperature in ambient air. The width of Hp film along SAW propagation was 3 mm, and the film thickness was on the order of microns, much less than the acoustic wavelength.

The samples ware placed into the closed chamber of about 5-liter volume. When the small piece of a wet paper was inserted into the chamber, the relative humidity (RH) slowly increased in time at the rate of a few % per minute. When the piece of a dry paper was inserted, the RH slowly decreased at a similar rate. The RH variations were monitored with the digital thermo-hygrometer RH411 (Omega Engineering, Inc.).

The transmission characteristics of the fabricated SAW structures were measured using the network analyzer E5062A (Agilent Technologies, Inc.). Fig. 4 shows the transmission loss dependence versus frequency f measured for the bare (without Hp layer) YZ-$LiNbO_3$ substrate. The calculated curve in Fig. 4 is based on the equivalent circuit of an IDT connected to the RF generator shown in Fig. 5 [9]. Based on this circuit, the SAW power can be expressed as:

$$P_a = \frac{1}{2}|U_a|^2 G_a , \tag{1}$$

where the voltage across radiation conductance is:

$$U_a = E\frac{\mathrm{Re}\,Z\left(R_s + \mathrm{Re}\,Z\right) + \left(\mathrm{Im}\,Z\right)^2 + j\,R_s\,\mathrm{Im}\,Z}{\left(R_s + \mathrm{Re}\,Z\right)^2 + \left(\mathrm{Im}\,Z\right)^2}, \tag{2a}$$

the IDT impedance is:

$$Z = \frac{G_a - j\left(B_a + \omega C_T\right)}{G_a^2 + \left(B_a + \omega C_T\right)^2}, \tag{2b}$$

E is the electromotive force and R_s is the intrinsic resistance of the RF generator. The factor ½ appears in Eq. 1 because only a half of SAW power radiated by the bidirectional IDT arrives to the receiving IDT.

The frequency dependent radiation conductance G_a and motional succeptance B_a of the IDT are expressed by well known expressions derived from the crossed-field model [10]:

$$G_a = 8K^2 f_0 C_T N\left|\frac{\sin X}{X}\right|^2, \tag{3a}$$

$$B_a = 8K^2 f_0 C_T N\,\frac{\sin(2X) - 2X}{2X^2}, \tag{3b}$$

where

$$X = \frac{N\pi\left(f - f_0\right)}{f_0}, \tag{3c}$$

K^2 is the electromechanical coupling constant, the IDT center frequency is

$$f_0 = \frac{V}{\Lambda}, \tag{3d}$$

V and Λ respectively are the SAW speed and the wavelength. The IDT static capacitance C_T can be expressed as

$$C_T = C_0 NW , \tag{3e}$$

where C_0 is the capacitance per single electrode pair of unit length, N is the number of electrode pairs, and W is the overlap length of IDT electrodes. Assuming that the energy conversion processes in both IDTs are reciprocal, the load resistance R_L of the receiving IDT is equal to R_s, and there

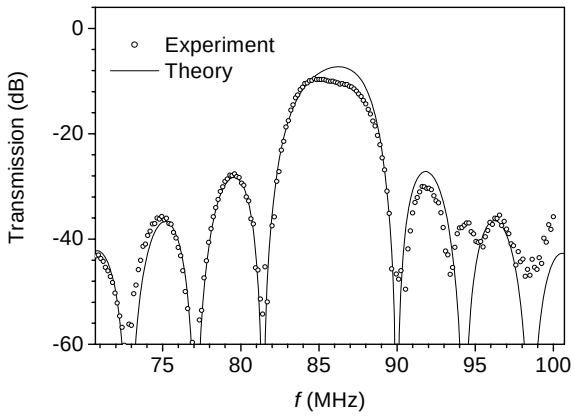

Fig. 4. **Experimental and theoretical transmission dependencies on frequency of SAW device on bare *YZ*-$LiNbO_3$ substrate**

is no propagation loss between two IDTs, one may express the transmission losses of the two-port SAW device as follows:

$$T = \left(4\frac{|U_a|^2}{E^2}G_a R_s\right)^2 . \tag{4}$$

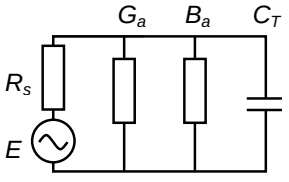

Fig. 5. **Equivalent circuit of IDT connected to RF source**

The calculation parameters K^2 = 4.5 %, and C_0 = 0.46 pF/mm for YZ-$LiNbO_3$ were taken from Ref. 9. For N = 20 and W = 2 mm one obtains C_T = 18.4 pF. As seen from Fig. 4, the measured and calculated (from Eq. 4) T (f) curves agree quite well.

No effect of the ambient humidity on the transmission characteristics was observed for bare *YZ*-$LiNbO_3$. In contrast, the SAW transmission characteristics of the samples with Hp layers strongly depended on a humidity. Fig. 6 shows the transmission characteristics of the Hp-$LiNbO_3$ SAW structure measured at different ambient humidity values. As seen, the hematoporphyrin layer introduces additional losses, which increase with increasing RH. At IDT center frequency 86 MHz, this increase is 4.5 dB, 11 dB, and 18.5 dB at RH = 13 %, 28 %, and 36 % respectively. We attribute this increase in transmission losses to the increase in SAW attenuation in hematoporphyrin layer as it adsorbs water from environment. The SAW attenuation extracted by dividing the loss change by the Hp layer length (3 mm in our case) is plotted in log scale as a function of a relative humidity in Fig. 7. As seen, the attenuation growth with RH can be well described by the exponential function 4.7 exp (RH/14.3).

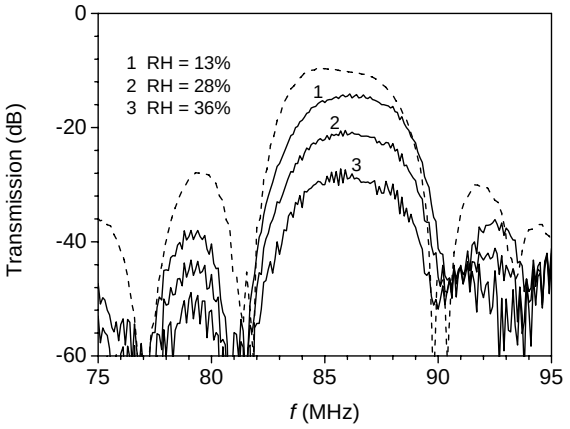

Fig. 6. **Transmission characteristics of Hp-$LiNbO_3$ SAW structure measured at different values of relative humidity (solid lines). The dashed line shows transmission characteristic for bare $LiNbO_3$ substrate.**

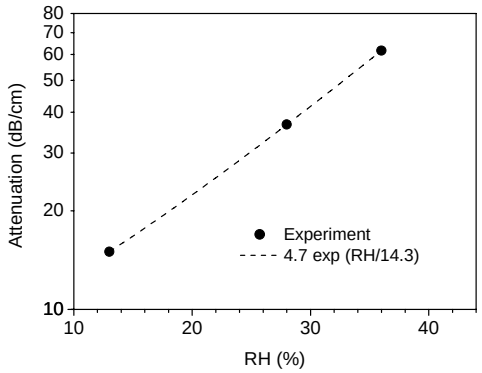

Fig. 7. **Dependence of SAW attenuation on a relative humidity in Hp-$LiNbO_3$ SAW structure at IDT center frequency 86 MHz. Dots – experiment; dashed line – exponential fit of the experimental dependence**

Next, the impact of ambient humidity on the SAW velocity in Hp-$LiNbO_3$ structure was investigated. For this purpose, we used the SAW-delay-line oscillator technique first described in [11]. The SAW delay-line oscillator consists of a wide-band RF amplifier with the SAW delay line connecting the amplifier input and output for a positive feedback. The custom-made RF amplifier was used in our experiment, and the Hp-$LiNbO_3$ structure under investigation was used as a positive-feedback element. More details on the SAW oscillator technique can be found in Ref. 12. Fig. 8 shows the image of the SAW-delay-line oscillator incorporating the Hp-$LiNbO_3$ sample

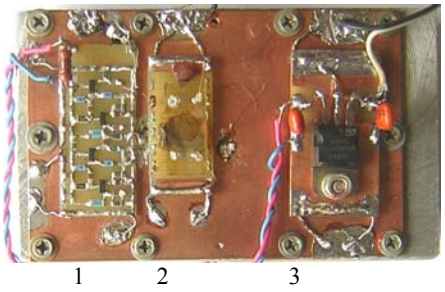

Fig. 8. **SAW delay-line oscillator: 1 - amplifier, 2 - Hp-$LiNbO_3$ sample, 3 - power supply**

is shown in. The fundamental frequency of the oscillator was 85 MHz. The oscillator was placed into the measuring chamber and the dependence of its oscillation frequency on ambient humidity was measured using the multi-function counter MS6100 (Mastech). Fig. 9 shows the measured change in the SAW oscillator frequency versus relative humidity with respect to the frequency value at RH = 9 %. With increasing humidity, the oscillator frequency decreases, and this decrease has a strongly non-linear character. The overall measured change in the frequency is about 30 kHz, i.e. 0.035 % of the fundamental frequency.

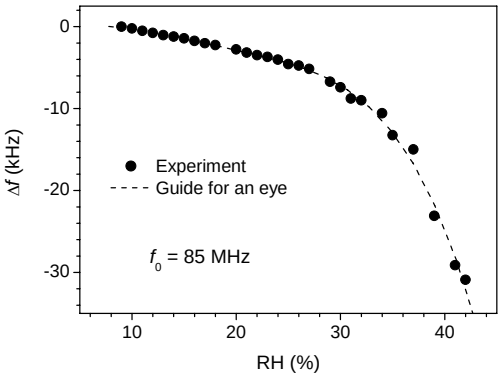

Fig. 9. **Change in SAW oscillator frequency versus ambient humidity**

No frequency dependence on humidity was observed for the SAW oscillator with a bare $LiNbO_3$ substrate. This confirms that the oscillator frequency variation is due to the moisture adsorption by Hp layer. We attribute this variation to the humidity-induced variation of the SAW velocity. The relative change in the SAW velocity can be extracted from the relative oscillator frequency change with the help of expression:

$$\frac{\Delta V}{V} = \frac{\Delta f}{f_0}\frac{L}{L_1}, \qquad (5)$$

where L is the center-to-center spacing between IDT transducers, and L_1 is the length of Hp layer along the

SAW propagation. In the sample investigated, L = 12 mm, and L_1 = 3 mm. The extracted dependence of relative velocity change (in log scale) on a relative humidity is plotted in Fig. 10. As seen, it can be satisfactory approximated by the exponential function 9.5 x 10^{-6} exp (RH/8.3).

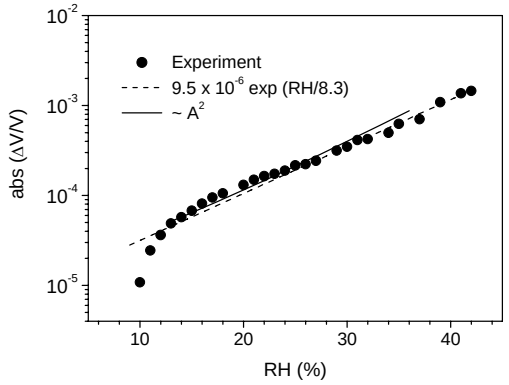

Fig. 10. **Relative change in SAW velocity versus ambient humidity at frequency 85 MHz. Dots – experiment; dashed line – exponential fit of experimental dependence; solid line – attenuation squared.**

We consider the change in Hp layer conductivity as a possible physical mechanism responsible for the observed changes in SAW attenuation and velocity. The dependence of the SAW attenuation on the layer sheet resistivity R_s is (see e.g. [13]):

$$A = 8.68\frac{K^2}{2}\frac{\omega}{V}\frac{\varepsilon_0\varepsilon V R_S}{1+(\varepsilon_0\varepsilon V R_S)^2} \qquad (6)$$

where ε is the effective dielectric constant, ε_0 is the permittivity of free space, and ω is the angular SAW frequency. When the sheet resistivity decreases from infinity to a finite R_s value, the corresponding SAW velocity change can be expressed as:

$$\frac{\Delta V}{V} = -\frac{K^2}{2}\frac{1}{1+(\varepsilon_0\varepsilon V R_s)^2}, \qquad (7)$$

If the condition $\varepsilon_0\varepsilon V R_S >> 1$ is satisfied,

$$A \sim 1/R_S\ ,\ \Delta V/V \sim 1/R_s^2\ .$$

Hence,

$$\Delta V/V \sim A^2\ . \qquad (8)$$

The slope of the dependence const·A^2(RH) for measured attenuation values is shown in Fig. 10. The constant was arbitrary chosen to fit the numerical value of $\Delta V/V$ at RH = 25 %. One can see that the experimental dependencies of SAW attenuation and relative velocity change are in good agreement with the relation (8). This confirms the assumption of a conductivity related mechanism of the humidity impact on the SAW propagation parameters in hematoporphyrin-lithium niobate structure.

Acknowledgements

The work at Vilnius University was partially supported by the Lithuanian State Science and Studies Foundation. The work at RPI was supported by ONR under the MURI program (Program manager Dr. Paul Maki).

References

1. **Yeo T. L., Sun T. and Grattan K. T.** V. Fibre-optic sensor technologies for humidity and moisture measurement. Sens. Actuators A. 2008. Vol.144. P.280-295.
2. **Lee C. Y. and Lee G. B.** Humidity sensors: a review. Sens. Lett. 2005. Vol.3. P.1-14.
3. **Cheeke J. D. N., Tashtoush N. and Eddy N.** Surface acoustic wave humidity sensor based on the change in the viscoelastic properties of a polymer film. IEEE Ultrason. Symp. Proc. 1996. P.449-452.
4. **Li Y., Yang M., Ling M. and Zhu Y.** Surface acoustic wave humidity sensors based on poly (p – diethynylbenzene) and sodium polysulfonesulfonate. Sens. Actuators B. 2007. Vol.122. P.560-563.
5. **Chen Z. and Lu C.** Humidity sensors: a review of materials and mechanisms. Sens. Lett. 2005. Vol.3. P.274-295.
6. **Rimeika R., Rotomskis R., Poderys V., Čiplys D., Sereika A., Selskis A. and Shur M. S**. Surface acoustic wave interaction with humidity sensitive $TPPS_4$ nano-strip structure. Ultragarsas. 2006. Vol.58. P.13-15.
7. **Rimeika R., Čiplys D., Poderys V., Rotomskis R., Balakauskas S. and Shur M. S.** Subsecond-response SAW humidity sensor with porphyrin nanostructure deposited on bare and metallised piezoelectric substrate. Electron. Lett. 2007. Vol.43. P.1055-1057.
8. **Brown S. B., Shillcock M. and Jones P.** Equilibrium and kinetic studies of the aggregation of porphyrin in aqueous solution. Biochem. J. 1976. Vol.153. P. 279-285.
9. **Campbell C. K.** Surface acoustic wave devices for mobile and wireless communications. Academic Press, San Diego. 1998.
10. **Smith W. R. , Gerard H. M., Collins J. H., Reeder T. M. and Shaw H. J.** Analysis of interdigital surface wave transducers by use of an equivalent circuit model. IEEE Trans. Microwave Technol. Techniques. 1969. Vol.17. P.856-864.
11. **Maines J. D., Paige E. G., Saunders A. F. and Young A. S.** Simple technique for the accurate determination of delay-time variations in acoustic-surface-wave-structures. Electron. Lett. 1969. Vol.26. P.678–680.
12. **Ciplys D., Rimeika R., Shur M. S., Rumyantsev S., Gaska R., Sereika A., Yang J. and Asif Khan M.** Visible-blind photoresponse of GaN-based surface acoustic wave oscillator. Appl. Phys. Lett. 2002. Vol.80. P. 2020-2022.
13. **Sivaramakrishnan S., Rajamani R., Smith C.S., McGee K. A., Mann K. R. and Yamashita N.** Carbon nanotube-coated surface acoustic wave sensor for carbon dioxide sensing. Sens. Actuators B. 2008. Vol.132. P. 296-304.

R. Rimeika, R. Rotomskis, V. Poderys, D. Čiplys, A. Sereika, M. S. Shur

Aplinkos drėgmės įtaka paviršinių akustinių bangų slopinimui ir greičiui hematoporfirino - $LiNbO_3$ dariniuose

Reziumė

Ištirtas aplinkos oro drėgmės poveikis paviršinių akustinių bangų (PAB) sklidimui darinyje iš hematoporfirino (Hp) sluoksnio, suformuoto ant pjezoelektrinio *YZ*-$LiNbO_3$ padėklo. Grandinių analizatoriumi išmatuotos darinio dažninės PAB perdavimo charakteristikos, o naudojant PAB vėlinimo linijos generatorių – PAB kreičio kitimas. Nustatyta, kad didėjant santykiniam drėgniui PAB slopinimas Hp sluoksnyje didėja, o greitis mažėja. Parodyta Hp-$LiNbO_3$ PAB linijos kaip drėgmės jutiklio taikymo galimybė.

Pateikta spaudai 2008 09 15